Monitoring stimulated emission at the single-photon level in one-dimensional atoms

Daniel Valente, Stefano Portolan, Gilles Nogues, Jean-Philippe Poizat,
Maxime Richard, Jean-Michel Gérard, Marcelo F. Santos, Alexia Auffèves

HAL Id: hal-00998935
https://hal.science/hal-00998935

Monitoring stimulated emission at the single-photon level in one-dimensional atoms

D. Valente,[1,*] S. Portolan,[1] G. Nogues,[1] J. P. Poizat,[1] M. Richard,[1] J. M. Gérard,[2] M. F. Santos,[3] and A. Auffèves[1]

[1]*Institut Néel–CNRS, Grenoble, France*

[2]*CEA/INAC/SP2M, Grenoble, France*

[3]*Universidade Federal de Minas Gerais, Belo Horizonte, Brazil*

We theoretically investigate signatures of stimulated emission at the single-photon level for a two-level atom interacting with a one-dimensional light field. We consider the transient regime where the atom is initially excited, and the steady-state regime where the atom is continuously driven with an external pump. The influence of pure dephasing is studied, clearly showing that these effects can be evidenced with state-of-the-art solid-state devices. We finally propose a scheme to demonstrate the stimulation of one optical transition by monitoring another one, in three-level one-dimensional atoms.

PACS number(s): 42.50.Ct, 42.50.Gy

I. INTRODUCTION

Exploration of the light-matter interaction at the single-photon level is a goal of quantum optics that has been successfully achieved so far with emitters in high-quality-factor microwave [1] or optical cavities [2]. High atom-field couplings are obtained at the price of keeping the photons trapped in the mode, which may limit their exploitation for all practical purposes. Alternative strategies have thus emerged, based on the coupling of the emitter to a one-dimensional (1D) electromagnetic environment. A pioneering realization of such a "1D atom" consisted in an atom coupled to a leaky directional cavity [3]. Nowadays, 1D atoms can be implemented in a wide range of physical systems, from quantum dots (QDs) embedded in photonic wires [4], in photonic crystals [5], or in plasmonic waveguides [6], to superconducting qubits in circuit QED [7,8], and to atoms [9] and molecules in tightly focused beams [10]. When probed with a resonant field, the natural directionality of 1D atoms allows a high mode matching to be reached between the incoming and the scattered light, manifested by the destructive interference of the two fields [5,8,10,11]. Equivalently, perfect mode matching allows saturation of the emitter with a single photon [11], so that 1D atoms have been identified as promising single-photon transistors [6] and two-photon gates [12].

This highly nonlinear behavior strongly motivates a study of the properties of the system when the atomic population is inverted and a reconsideration in the one-dimensional geometry of the concept of stimulated emission introduced by Einstein [13]. A search for signatures of stimulation at the single-photon level not only provides new insights into a fundamental concept of quantum optics, but also allows the envisioning of appealing applications in quantum information processing. Optimal quantum cloning machines and single-photon adders could be implemented in these systems and offer promising alternatives to devices based on cavity quantum electrodynamics, where these functionalities have been probed so far [14,15]. In this paper we theoretically characterize

stimulation by single photons in two different regimes, namely, the transient regime where the atom is initially excited and the steady-state regime where the emitter is continuously excited by an incoherent light source. Signatures of stimulated emission are sought in the atomic population and in the light field radiated by the atom. To study the potential of solid-state systems to demonstrate such effects, pure dephasing is taken into account. Finally, the possibility of exploiting an ancillary atomic transition to monitor the stimulation is explored.

II. MODEL

The scheme of a two-level emitter of frequency ω_A interacting with a continuum of modes inside a 1D waveguide is pictured in Fig. 1(a). The quantized field in the Heisenberg picture is written $E(z,t) = E^{(+)}(z,t) + E^{(-)}(z,t)$ [16], where $E^{(+)}(z,t) = i \sum_\omega \epsilon_\omega \{a_\omega(t) e^{ikz} + b_\omega(t) e^{-ikz}\}$. We have explicitly separated the forward a_ω from the backward b_ω propagating modes [17]. The electric field per photon is ϵ_ω. The atomic emission is eventually stimulated by a laser of frequency ω_L injected into the waveguide. This is well described by a coherent field α_L in the guided mode of the same frequency, the other modes being in the vacuum [18]. The coupling Hamiltonian between the field and the atomic dipole written in the rotating-wave approximation is $H_I = -i\hbar \sum_\omega g_\omega[\sigma_+(a_\omega e^{i(\omega/c)z_A} + b_\omega e^{-i(\omega/c)z_A}) - \text{H.c.}]$, where z_A is the position of the atom inside the waveguide, which we further take equal to 0. The atomic operators are denoted $\sigma_+ = |e\rangle\langle g|$, $\sigma_- = \sigma_+^\dagger$, and $\sigma_z = (\sigma_+\sigma_- - \sigma_-\sigma_+)/2$. The coupling frequency is defined by $g_\omega = d\epsilon_\omega/\hbar$, where d is the electric dipole between $|g\rangle$ and $|e\rangle$ states. In addition to the Hamiltonian part, an incoherent pump ξ can be added to invert the atomic population. As pictured in Fig. 1, such a mechanism is obtained by resonantly pumping an ancilla level $|m\rangle$ that immediately decays toward the excited level $|e\rangle$. We also include a pure dephasing rate γ^* [19,20], related to electrostatic fluctuations of the environment [21], usually present in solid-state artificial atoms. The total decay rate is $\gamma = \gamma_0 + \gamma_1$, where γ_1 is the relaxation rate due to the coupling with the 1D continuum. Unavoidable coupling to
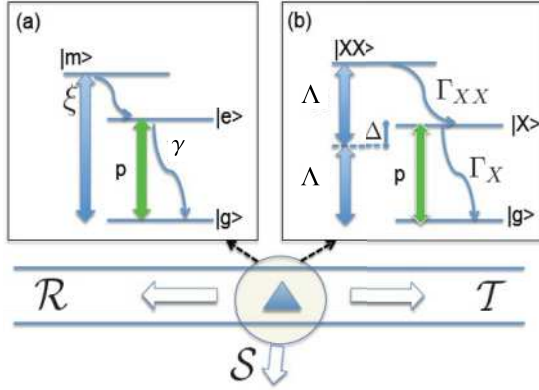
*daniel.valente@grenoble.cnrs.fr

FIG. 1. (Color online) Level scheme of the 1D atom under study under (a) incoherent pumping or (b) coherent two-photon excitation in the QD case. The notations are introduced in the text.

the other modes of the 3D electromagnetic environment gives rise to the additional rate γ_0. The time evolution of the operators is given by a set of coupled Heisenberg-Langevin equations, written in the frame rotating at the laser frequency in the Markovian approximation [17,18]. This leads to the following set of equations, valid in the 1D geometry:

$$\frac{d}{dt}\langle\sigma_-\rangle = -\left(\frac{\gamma + \gamma^* + \xi}{2} - i\delta_L\right)\langle\sigma_-\rangle + \Omega\langle\sigma_z\rangle,$$

$$\frac{d}{dt}\langle\sigma_z\rangle = -(\gamma + \xi)\left(\langle\sigma_z\rangle + \frac{1}{2}\right) + \xi - \Omega\,\mathrm{Re}[\langle\sigma_-\rangle], \tag{1}$$

where $\delta_L = \omega_L - \omega_A$ is the detuning between the atom and the laser and Re stands for the real part. In the following, we will always consider the resonant case, $\delta_L = 0$. The Rabi frequency Ω characterizes the coupling between the atom and the field and equals $\Omega = \gamma\sqrt{2\beta}\sqrt{p}$, where $p = |\alpha_L|^2/(\pi\rho_{1_D}\gamma)$ is the number of incoming photons per atomic lifetime, $\rho_{1_D} = L/\pi c$ is the density of modes of the continuum with length of quantization L, and $\beta = \gamma_1/(\gamma_0 + \gamma_1)$ quantifies the 1D character of the system. An ideal 1D atom corresponds to $\beta = 1$, a limit almost reached in circuit QED [8]. Other experimental setups also provide nearly ideal 1D systems, namely, atoms in strongly dissipative cavities ($\beta = 0.96$ [3]), and QDs in photonic nanowires ($\beta = 0.95$ [4]) or in photonic-crystal waveguides ($\beta = 0.98$ [5]).

As far as the light field is concerned, we derive the photodetection relation proper to the 1D geometry, valid for all z and $t > |z|/c$:

$$E^{(+)}(z,t) = E_{a,\mathrm{free}}(z,t) + E_{b,\mathrm{free}}(z,t)$$
$$+ \eta\left\{\sigma_-\left(t - \frac{z}{c}\right)\Theta(z) + \sigma_-\left(t + \frac{z}{c}\right)\Theta(-z)\right\}, \tag{2}$$

where we have introduced the parameter $\eta = i\epsilon_{\omega_L}\sqrt{\beta/2}$. The counterpropagating free field operators are $E_{a,\mathrm{free}}(z,t) = i\sum_\omega \epsilon_\omega a_\omega(0)e^{-i\omega(t-z/c)}$ and $E_{b,\mathrm{free}}(z,t) = i\sum_\omega \epsilon_\omega b_\omega(0)e^{-i\omega(t+z/c)}$. Finally, the expressions for the powers $\gamma\langle E^{(-)}E^{(+)}\rangle/\epsilon_{\omega_L}^2$ radiated in the transmission and
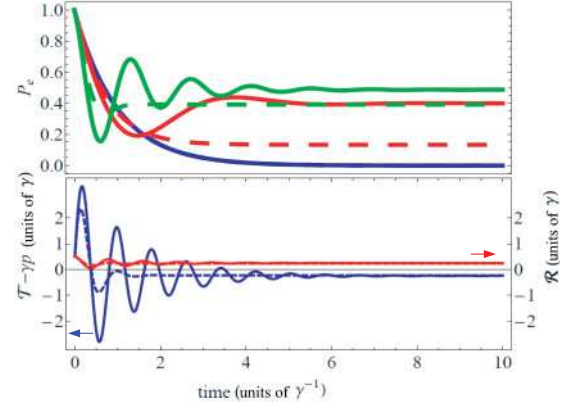

FIG. 2. (Color online) Top: Excited-state population $P_e(t)$ as a function of time (in units of γ^{-1}) for $p = 0$ (blue, monotonic decrease), $p = 1$ (red, lower-frequency oscillation), and $p = 10$ (green, higher-frequency oscillation). Bottom: $\mathcal{T} - \gamma p$ (blue, left arrow) and $\mathcal{R}$ (red, right arrow; both in units of γ) for $p = 30$, showing that net transmission overcomes reflection whenever stimulated emission takes place, in the transient regime. Dashed curves correspond to $\gamma^* = 10\gamma$. For all cases, $\beta = 1$.

reflection channels, respectively denoted $\mathcal{T}$ and $\mathcal{R}$, are expressed in numbers of photons per second and read

$$\mathcal{T} = \gamma p + \Omega\,\mathrm{Re}[\langle\sigma_-\rangle] + \frac{\gamma\beta}{2}\left(\langle\sigma_z\rangle + \frac{1}{2}\right), \tag{3}$$

$$\mathcal{R} = \frac{\gamma\beta}{2}\left(\langle\sigma_z\rangle + \frac{1}{2}\right), \tag{4}$$

whereas the power dissipated in the leaky modes is denoted $\mathcal{S}$ and is given by $\mathcal{S} = \gamma(1-\beta)\left(\langle\sigma_z\rangle + \frac{1}{2}\right)$. The first term in $\mathcal{T}$ equals the incoming laser power γp. The last term is due to spontaneous emission and equally contributes to $\mathcal{R}$ and $\mathcal{T}$. It scales as the excited population $P_e = \langle\sigma_z\rangle + 1/2$, so that this atomic observable can be continuously monitored by observing the reflection $\mathcal{R}$ or the leaky channel $\mathcal{S}$. The interference term $\Omega\mathrm{Re}[\langle\sigma_-\rangle]$ plays a key role in the 1D geometry under study. It equals $\mathcal{T} - \gamma p - \mathcal{R}$, allowing one to compare the net transmitted power $\mathcal{T} - \gamma p$ to the reflected power $\mathcal{R}$. Thus it quantifies the preferred emission channel. This quantity also acts on the evolution of the population P_e as it appears in Eq. (1). Following the notations of a seminal paper by Mollow [22], this term exactly satisfies $\Omega\mathrm{Re}[\langle\sigma_-\rangle] = -\mathcal{W}[p]$, where $\mathcal{W}[p]$ stands for the coherent atomic absorption.

III. TRANSIENT REGIME

We first consider the transient regime where the incoherent pump is switched off ($\xi = 0$), and the atom initially prepared in the excited state $|e\rangle$ is driven by a cw resonant field p. The evolution of the population $P_e(t)$ is given by solving Eqs. (1), which correspond to standard Bloch equations in the case $\xi = 0$ under study. It is plotted in Fig. 2 with $\beta = 1$. The case $p = 0$ corresponds to the damped regime. It is characterized by an exponential decay, typical for the spontaneous emission of a photon into the waveguide. As can be seen in the figure, increasing the pump power stimulates this emission. However,

it appears that stimulated emission does not make the atomic decay faster, but reversible: this is the nonlinear regime of Bloch equations, characterized by the coherent exchange of photons between the atom and the field (Rabi oscillations) at the rate Ω. This regime is reached when Ω overcomes the typical dephasing and damping rates γ and γ^*. When $\gamma^* = 0$, this condition simplifies to $p \propto \beta^{-1}$ [see Eq. (1)], which corresponds to $p \sim 1$ in the ideal 1D case plotted in the figure. Therefore, a single photon per lifetime is enough to saturate a 1D atom, as already evidenced in a different context [11,12]. If $\beta < 1$, a higher pump power will be necessary to reach the nonlinear regime. Single-photon sensitivity is also altered by pure dephasing, as is shown in Fig. 2 where we have plotted the population with $\gamma^* = 10\gamma$, a typical value for quantum dots [20] (note that this is an upper bound, pure dephasing rates as low as $\gamma^* = 0.15\gamma$ being currently reached in circuit QED [8]). Still, it appears that with realistic parameters, the power needed to reach stimulation remains of the order of a few photons per lifetime, so that the great sensitivity of the device is preserved. Finally, note that the observed Rabi oscillation is classical and does not lead to any entanglement with the field, in contrast to the case of an atom coupled to a monomode cavity [1], another medium showing single-photon sensitivity. In that sense, 1D geometry is similar to low-quality-factor Ramsey zones used in microwave cavity QED experiments [23].

It is also interesting to observe the evolution of the radiated fields in the regime of stimulated emission. This is plotted in Fig. 2 for $p = 30$. Rabi oscillations are also visible in the reflected and transmitted fields. In particular, one observes that each decrease in $\mathcal{R}$ corresponds to the stimulated emission of a photon, which feeds the transmission channel. These processes have $\mathcal{T} - \gamma p > \mathcal{R}$, confirming that the "stimulated channel" $\mathcal{T}$ is favored. Note that, on the other hand, if the atom is initially prepared in the ground state $|g\rangle$, emission is favored in the reflection channel at the initial time, a property that can be exploited to develop single-photon transistors [6,10].

IV. STEADY-STATE REGIME

Let us now concentrate on the case where the atom is continuously driven by an incoherent pump ξ and study the influence of the resonant light on the steady-state atomic population P_e and radiated fields $\mathcal{R}$ and $\mathcal{T} - \gamma p$. The population is pictured in Fig. 3 as a function of p. We have plotted the results for two different values of the incoherent pump $\xi = 3\gamma$ and 15γ, yielding two different population inversions ($P_e > P_g$) when $p = 0$. We also show the net total rate of photons emitted by the atom, $N = \mathcal{T} - \gamma p + \mathcal{R} + \mathcal{S}$. Moreover, we have defined and plotted the ratios β_R (β_T) of photons emitted in the reflection (transmission) channel in the following way: $\beta_R = \mathcal{R}/N$, $\beta_T = (\mathcal{T} - \gamma p)/N$. These quantities measure the propensity of the atom to emit in the reflection (transmission) channels and appear as natural figures of merit for stimulated emission. Two regimes can be observed in the figure. A vanishing pump $p \rightarrow 0$ gives rise to an incoherent regime characterized by the spontaneous emission of photons. The excited-state population reads $P_e = \frac{\xi}{\gamma + \xi}$ and the net total rate of emitted photons is $N = \gamma P_e$. In this regime, no channel is favored, and the net transmitted and reflected fields are equal. Increasing the pump
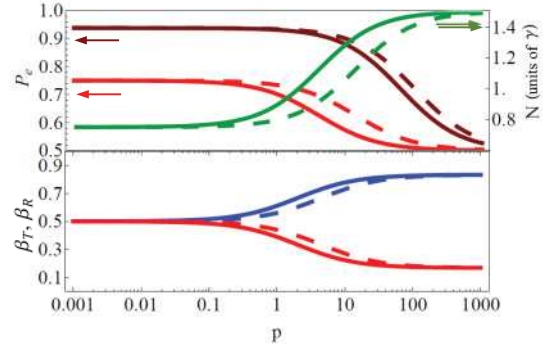

FIG. 3. (Color online) Top: Steady-state population (red, left arrows) of the excited level (proportional to reflected power) as a function of the resonant pump for $\xi = 3\gamma$ (light red, lower) and 15γ (dark red, upper). Increasing net rate of emitted photons N (green, right arrow; in units of γ) ranging from γP_e to $\xi/2$ (plotted with $\xi = 3\gamma$). Bottom: Ratios β_T (blue, upper) and β_R (red, lower) showing predominance of emission in the transmission channel for $p > 1$. Dashed curves: $\gamma^* = 10\gamma$. We took $\beta = 1$.

p to arbitrarily high values sets up the coherent regime of Rabi oscillations. The excited-state population P_e decreases, eventually becoming equal to the ground-state population P_g, which is the usual limit of Bloch equations when the atom is saturated [18]. Simultaneously, the net total rate of photons increases to $N = \xi/2$. This is an unusual situation where the emitted light power does not follow the same evolution as the atomic population. As a matter of fact, the rate N represents the rate of photons exchanged between the atom and the field, which scales as the Rabi frequency Ω and increases with the pump power p. Simultaneously, the transmission channel is markedly favored with respect to the reflection channel ($\beta_T > \beta_R$). The transition between these two regimes happens when $p > p_{\text{th}} = \frac{(\gamma + \gamma^* + \xi)(\gamma + \xi)}{4\beta\gamma^2}$, which simplifies to $p_{\text{th}} = \frac{1}{4}(1 + \frac{\xi}{\gamma})^2$ for $\beta = 1$ and $\gamma^* \ll \gamma$. This confirms that Rabi oscillations appear when coherent processes, quantified by p, overcome incoherent ones, quantified by ξ. As in the transient case, pure dephasing and lower β increase the threshold needed to reach the coherent regime, up to values that remain of the order of a few photons per lifetime in the physical systems modeled.

V. EXPERIMENTAL PROPOSAL FOR INDIRECT MEASUREMENT OF STIMULATED EMISSION

Measurement of the ratios β_R and β_T is experimentally quite demanding. As a matter of fact, it requires the ability to quantify the total power radiated by the atom, in particular the net transmitted power $\mathcal{T} - \gamma p$, and hence to filter the pump to extract a tiny atomic emission. Therefore, we propose an experimentally feasible way to measure this quantity, by exploiting a third atomic level $|XX\rangle$ as pictured in Fig. 1(b). This three-level structure can model the biexcitonic and the excitonic transitions of a quantum dot, a terminology that we shall use from now on without losing the generality of the scheme. Population inversion on the excitonic transition ($P_X > P_g$) is reached by resonantly pumping a biexciton in the dot using the two-photon-absorption technique. This
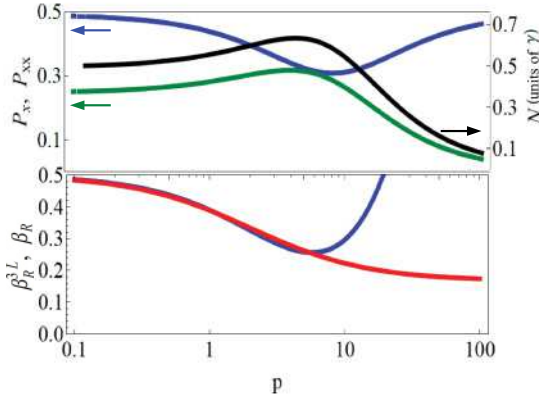
FIG. 4. (Color online) Top: Populations (left arrows) P_X (blue, upper) and P_{XX} (green, lower) of the three-level system vs p. Net rate of photon emission N (black, right arrow; in units of γ) in the exciton transition. Bottom: Comparison between the ratios of emission given by the two (β_R, red, lower) and three (β_R^{3L}, blue, upper) levels, assuming $\xi \sim 3\gamma$ and $\Lambda^2/\Delta \sim 4\Gamma_X$. In both cases, $\gamma^* = 0$ and $\beta = 1$.

mechanism can be described by an effective Hamiltonian $H_{2\mathrm{ph}} = \hbar \Lambda^2/\Delta (|XX\rangle\langle g|\ e^{-i\nu t} + \mathrm{H.c.})$, where $\Delta = (E_{XX} - E_X)/2$ and Λ is the Rabi frequency of the pump [24]. As usual, Lindbladians describe the decays $|XX\rangle \rightarrow |X\rangle$, with rate Γ_{XX}, and $|X\rangle \rightarrow |g\rangle$, with rate Γ_X. The populations of the excitonic P_X and biexcitonic states P_{XX} are computed in the steady-state regime, as a function of the resonant probe p. The results are plotted in Fig. 4. When $p = 0$, the presence of a large pump power $\Lambda^2/\Delta > \Gamma_{XX}$ leads to equalization of the populations of the ground and biexcitonic states, whereas detailed balance conditions require $P_X/P_{XX} = \Gamma_{XX}/\Gamma_X$. The usual quantum dot parameters satisfy $\Gamma_{XX} \approx 2\Gamma_X$ [4], leading to $P_{XX} = P_g = 1/4$ and $P_X = 1/2$. Increasing the probe power p leads to the depletion of the excitonic level because of stimulated emission, and thus to the increase of the steady-state biexcitonic population, as is shown in Fig. 4. This increase can be monitored by measuring the rate of photon emission $\Gamma_{XX} P_{XX}$ at the biexcitonic frequency, which provides an easily observable signature of stimulated emission at the single-photon level. Moreover, we have verified that $\Gamma_{XX} P_{XX} = \Gamma_X P_X - \mathcal{W}[p] = N$, where $\mathcal{W}[p]$ is the interference term between the probe and the light emitted at the excitonic frequency, as defined above. Namely, the rate of photon emission in the biexcitonic line exactly equals the rate N emitted in the excitonic one,

taking into account stimulated processes. Stimulated emission of the excitonic transition can thus be simply monitored by measuring the rate of photon emission at the biexcitonic frequency. This rate can be used to build the ratio β_R defined above, without having to measure the net transmitted power. This is also represented in Fig. 4, where we have plotted $\beta_R^{3L} = \frac{\frac{\Gamma_X}{2} P_X}{\Gamma_{XX} P_{XX}}$, the index $3L$ standing for three levels. For the sake of comparison, we have plotted on the same figure the quantity β_R defined in the case of a two-level atom. The equivalence between the models is clearly shown in the coincidence of the two curves for low power p ($\Omega = \gamma \sqrt{\beta}\sqrt{2p} < \Lambda^2/\Delta$). A divergence becomes unavoidable when p is strong enough to generate Autler-Townes splitting [25] of the ground level. The biexcitonic transition thus becomes out of resonance with the Λ driving field. So the population of the biexciton state drastically decreases, making the ratio β_R^{3L} arbitrarily large and equalizing exciton and ground-state populations. A possible drawback of experiments performed with quantum dots can be imperfect two-photon absorption, leading to incoherent feeding of the excitonic level via phonons, even for large Δ [26]. However, a recent experimental work [27] shows that the two-photon transition can be made very clean, so that the incoherent exciton pumping is negligible in this case. Finally, note that a scheme to fully protect entanglement has been proposed using the same mechanism of biexcitonic pumping and readouts of the light emitted in each possible transition [28].

VI. CONCLUSION

In conclusion, we have evidenced signatures of stimulated emission at the single-photon level, giving rise to potentially observable effects with state-of-the-art solid-state atomic devices interacting with 1D light fields. In particular, we propose an experiment to probe the stimulated (optical) transition, based on the monitoring of an ancillary transition. Properties of 1D atoms evidenced in this work may be exploited to implement fundamental quantum tasks, such as single-photon optimal cloning or single-photon amplification.

ACKNOWLEDGMENTS

[1] M. Brune, F. Schmidt-Kaler, A. Maali, J. Dreyer, E. Hagley, J. M. Raimond, and S. Haroche, Phys. Rev. Lett. **76**, 1800 (1996).

[2] A. Boca, R. Miller, K. M. Birnbaum, A. D. Boozer, J. McKeever, and H. J. Kimble, Phys. Rev. Lett. **93**, 233603 (2004).

[3] Q. A. Turchette, C. J. Hood, W. Lange, H. Mabuchi, and H. J. Kimble, Phys. Rev. Lett. **75**, 4710 (1995); Q. A. Turchette, R. J. Thompson, and H. J. Kimble, Appl. Phys. B **60**, S1 (1995).

[4] J. Claudon, J. Bleuse, N. S. Malik, M. Bazin, P. Jaffrennou, N. Gregersen, C. Sauvan, P. Lalanne, and J.-M. Gérard, Nat. Photonics **4**, 174 (2010).

[5] D. Englund, A. Faraon, I. Fushman, N. Stoltz, P. Petroff, and J. Vukovi, Nature (London) **450**, 857 (2007).

[6] D. E. Chang, A. S. Sorensen, E. A. Demler, and M. D. Lukin, Nat. Phys. **3**, 807 (2007).

[7] R. J. Schoelkopf and S. M. Girvin, Nature (London) **451**, 664 (2008).

[8] O. Astafiev, A. M. Zagoskin, A. A. Abdumalikov Jr., Yu. A. Pashkin, T. Yamamoto, K. Inomata, Y. Nakamura, and J. S. Tsai, Science **327**, 840 (2010).

[9] S. A. Aljunid, M. K. Tey, B. Chng, T. Liew, G. Maslennikov, V. Scarani, and C. Kurtsiefer, Phys. Rev. Lett. **103**, 153601 (2009); M. Stobinska, G. Alber, and G. Leuchs, Europhys. Lett. **86**, 14007 (2009).

[10] G. Wrigge, I. Gerhardt, J. Hwang, G. Zumofen, and V. Sandoghdar, Nat. Phys. **4**, 60 (2008); J. Hwang, M. Pototschnig, R. Lettow, G. Zumofen, A. Renn, S. Götzinger, and V. Sandoghdar, Nature (London) **460**, 76 (2009).

[11] A. Auffeves-Garnier, C. Simon, J. M. Gerard, and J. P. Poizat, Phys. Rev. A **75**, 053823 (2007).

[12] K. Kojima, H. F. Hofmann, S. Takeuchi, and K. Sasaki, Phys. Rev. A **70**, 013810 (2004).

[13] A. Einstein, Phys. Z. **18**, 121 (1917).

[14] C. Simon, G. Weihs, and A. Zeilinger, Phys. Rev. Lett. **84**, 2993 (2000).

[15] G. Rempe, F. Schmidt-Kaler, and H. Walther, Phys. Rev. Lett. **64**, 2783 (1990).

[16] R. J. Glauber, Phys. Rev. **130**, 2529 (1963).

[17] P. Domokos, P. Horak, and H. Ritsch, Phys. Rev. A **65**, 033832 (2002).

[18] C. Cohen-Tannoudji, J. Dupont-Roc, and G. Grynberg, *Atom-Photon Interactions: Basic Processes and Applications*, 2nd ed. (Wiley, New York, 2004).

[19] H. Carmichael, *An Open System Approach to Quantum Optics* (Springer-Verlag, Berlin, 1993).

[20] A. Auffeves, J. M. Gerard, and J. P. Poizat, Phys. Rev. A **79**, 053838 (2009).

[21] I. Favero, A. Berthelot, G. Cassabois, C. Voisin, C. Delalande, P. Roussignol, R. Ferreira, and J. M. Gerard, Phys. Rev. B **75**, 073308 (2007).

[22] B. R. Mollow, Phys. Rev. A **5**, 2217 (1972).

[23] J. I. Kim, K. M. Fonseca Romero, A. M. Higuti, L. Davidovich, M. C. Nemes, and A. F. R. de Toledo Piza, Phys. Rev. Lett. **82**, 4737 (1999).

[24] M. Brune, J. M. Raimond, and S. Haroche, Phys. Rev. A **35**, 154 (1987); E. del Valle, S. Zippilli, F. P. Laussy, A. Gonzalez-Tudela, G. Morigi, and C. Tejedor, Phys. Rev. B **81**, 035302 (2010).

[25] S. H. Autler and C. H. Townes, Phys. Rev. **100**, 703 (1955).

[26] K. Brunner, G. Abstreiter, G. Bohm, G. Trankle, and G. Weimann, Phys. Rev. Lett. **73**, 1138 (1994); M. Winger, T. Volz, G. Tarel, S. Portolan, A. Badolato, K. J. Hennessy, E. L. Hu, A. Beveratos, J. Finley, V. Savona, and A. Imamoğlu, *ibid.* **103**, 207403 (2009).

[27] T. Flissikowski, A. Betke, I. A. Akimov, and F. Henneberger, Phys. Rev. Lett. **92**, 227401 (2004).

[28] A. R. R. Carvalho and M. F. Santos, New J. Phys. **13**, 013010 (2011).